Society For Biomaterials

The influence of substrate modulus on retinal pigment epithelial cells

Corina White,[1] Tyler DiStefano,[2] Ronke Olabisi[3]

[1]Biomedical Engineering, The State University of New Jersey, Rutgers University, Piscataway, New Jersey
[2]Neurobiology, Neurodegeneration, and Repair, National Eye Institute, Bethesda, Maryland
[3]Biomedical Engineering, Rutgers University, Piscataway, New Jersey

Received 26 May 2016; revised 3 December 2016; accepted 21 December 2016
Published online 13 February 2017 in Wiley Online Library (wileyonlinelibrary.com). DOI: 10.1002/jbm.a.35992

Abstract: Although transplantation of retinal pigment epithelial (RPE) cells has shown promise for the treatment of retinal degenerative diseases, this therapeutic approach is not without challenges. Two major challenges are RPE cell dedifferentiation and inflammatory response following transplantation. The aim of this work is to understand how the rigidity of a scaffold, a relatively unexplored design aspect in retinal tissue engineering, affects RPE cells, particularly the pathways associated with the aforementioned challenges. Poly(ethylene glycol) diacrylate (PEGDA) of varying molecular weights from 3.4 to 20 kDa were photopolymerized to fabricate scaffolds. The Young's modulus of the scaffolds varied from 60 to 1200 kPa. A cell study was then conducted to test the effects of scaffold rigidity on RPE cells. A cell adhesion peptide motif of arginine-glycine-aspartic acid-serine (RGDS) was conjugated to 60 and 1200 kPa scaffolds and ARPE-19 cells, a human RPE cell line, were seeded onto these hydrogels. Cells grown on scaffolds demonstrated qualitatively different adhesion properties, metabolic activity, and gene expression at an mRNA level. IL-6 and MCP-1, two inflammation markers known to recruit microglial into the retina, had the same expression pattern with cells having the highest expression on the high modulus scaffold and lowest expression on the control substrate. This study demonstrates that scaffold rigidity, an important design parameter in other areas of tissue engineering, affects cell adhesion, activity, and expression of RPE cells. Though more exploration is needed, this begins to lay a foundation for optimizing scaffold rigidity to promote long-term success of RPE scaffolds. © 2017 The Authors *Journal of Biomedical Materials Research Part A* Published by Wiley Periodicals, Inc. J Biomed Mater Res Part A: 105A: 1260–1266, 2017.

Key Words: retinal pigment epithelium, Bruch's membrane, modulus

How to cite this article: White C, DiStefano T, Olabisi R. 2017. The influence of substrate modulus on retinal pigment epithelial cells. J Biomed Mater Res Part A 2017:105A:1260–1266.

INTRODUCTION

Age-related macular degeneration (AMD) is the leading cause of blindness in developed countries. With the aging population, the number of people affected by this disease is expected to triple over the next 30–40 years. Since the macula is responsible for central vision, its degeneration in AMD results in central vision loss. There are two forms of this disease. The first, wet AMD, is caused by neovascularization of the retina which leaks fluid into the macula, disrupting the retinal microenvironment. The second form, dry AMD, which accounts for up to 85% of clinical cases, is characterized by geographic atrophy of the retinal cells in the retina.[1] Retinal pigment epithelium (RPE) dysfunction occurs early in dry AMD. Healthy RPE supports the viability and function of photoreceptors, neural retinal cells, and choroidal vasculature. However, in dry AMD, the RPE loses its competence to support other retinal cell types, which contributes to photoreceptor degeneration and loss of visual acuity. Wet AMD is currently treated with photodynamic or photocoagulation treatment, whereby lasers are used to seal the vasculature that is leaking into the eye, or pharmaceutical intervention to inhibit blood vessel formation. These treatments require repeated applications as recurrence is common. Dry AMD makes up a majority of all clinical cases, and there are currently no effective therapeutic options. The only approaches in treating dry AMD are dietary changes and/or the addition of dietary supplements; however, these strategies have not proven to be significantly effective.[2]

Because of its critical role in maintaining a healthy retina and its apparent dysfunction in AMD, the RPE has become an attractive target for therapies, specifically cell therapies.[3] For decades, the field has implanted free cells subretinally and demonstrated the promise of cell therapy.[4–8] However, any positive results are mostly in the short term with results from long-term studies showing poor outcomes.[9] This is likely due to the fact that other underlying problems are not addressed; free cell injections replace lost cells but do nothing to repair the aged and diseased host environment. In the aged retina, there are alterations to the Bruch's membrane (BM), the acellular membrane upon

Correspondence to: Corina Elizabeth White; e-mail: corina.white@rutgers.edu
Contract grant sponsor: NIGMS (Rutgers Biotechnology Training Program); contract grant number: Ruth L. Kirschstein National Research Service Award T32 GM8339

which the RPE sits. These changes include increased thickness, a higher level of collagen crosslinking, the accumulation of waste and extracellular material known as drusen, and coated lipid bodies both within the BM and under the RPE.[10] These alterations in the BM are significant, as studies have demonstrated poor adhesion, gene expression, and RPE function on aged BM.[11,12] There is also insufficient solute transport through the diseased BM. Therefore, a successful therapy must address both the dysfunctional RPE and the aged BM. This has motivated cell therapy researchers to develop scaffolds for the implantation of RPE cells.

Several materials have been used to fabricate scaffolds for RPE delivery. These include both natural and synthetic polymers. These scaffolds show positive results *in vitro*, successfully maintaining viable RPE cells capable of forming monolayers with tight junctions and phagocytic ability.[13–17] Despite these *in vitro* successes, there are still challenges that must be addressed upon implantation of cell-seeded scaffolds. First, a common occurrence following scaffold implantation is that the immune cells of the nervous system, the microglia, begin to appear in the neural retina and are accompanied by the formation of a microglial scar on the retinal side of the scaffold.[18] This microglial migration is an inflammatory response triggered by interleukin 6 (IL-6) and monocyte chemoattractant protein-1 (MCP-1) in the retina. A microglial scarring response, particularly in neural implants, decreases implant efficacy.[19,20] Second, RPE cells have the capacity to dedifferentiate or transdifferentiate into a macrophage- or fibroblast-like phenotype through the SMAD3 pathway.[21] These dedifferentiated phenotypes lose the functionality of a mature RPE cell. The dedifferentiated phenotypes are commonly seen *in vivo* following scaffold-cell implantation.[18,22–24]

Scaffold substrate modulus has been demonstrated to affect cell adhesion, migration, expression, and function in a variety of cells.[25–27] However, in the majority of previously published scaffolds for RPE transplantation, scaffold modulus has largely been neglected as a design parameter. Substrate modulus is an especially important parameter for anchorage-dependent cells such as RPE cells. RPE cells' dependence on adhesion to a matrix is so great that once detached, they are known to initiate anoikis—cell death due to detachment. In a Science review, Discher et al. discuss the key roles in molecular pathways played by adhesion complexes and the cytoskeleton of many different cell types, including epithelial cells.[28] Pelham et al. performed one of the first studies to understand the effects of scaffold modulus and used epithelial cells and fibroblastic cells on polyacrylamide hydrogels of varying modulus.[29] Compared with cells on stiff gels, those on softer, more compliant substrates showed reduced cell spreading, higher rates of motility, and more dynamic cell adhesions. Because it has been established that RPE adhesion is altered on aged BM, which is known to have an altered modulus, and that during RPE dedifferentiation a change in the expression of cytokeratins (a component of the intracellular cytoskeleton) is observed, understanding how the modulus of a scaffold affects RPE cells may lead to better design of scaffolds and improve the *in vivo* fate of seeded RPE cells.

Towards that end, we investigate the effects of changing the modulus of a synthetic scaffold on seeded RPE cells. Poly(ethylene glycol) diacrylate (PEGDA) is a highly bioinert synthetic polymer with tunable mechanical properties.[30] Often referred to as a blank slate, the lack of any substantive biological cues in PEGDA hydrogels permits the evaluation of scaffold modulus on RPE cells without other confounding variables. By functionalizing PEGDA with the cell adhesion protein sequence, RGDS, we were able to isolate and systematically study how the elastic modulus of a scaffold affects the viability, cell adhesion, metabolic activity, and gene expression of RPE cells.

METHODS

All reagents were purchased from Sigma-Aldrich (Saint Louis, MO) and used as obtained without further purification unless otherwise noted.

Scaffold preparation for mechanical testing

Hydrogel scaffolds were prepared using a polymer solution containing one of four different molecular weight PEGDA (Laysan Bio, Arab, AL) in HEPES-buffered saline (10 m*M* *N*-[2-hydroxyethyl]piperazine-N0-[2-ethanesulfonic acid] and NaCl in ultra pure water), with 10 μL/mL photoinitiator solution (2,2-dimethoxy-2-phenyl-acetophenone 300 mg/mL in *N*-vinylpyrrolidone). The four molecular weights of PEGDA used were 3.4, 5, 10, and 20 kDa. The concentrations used for 10 and 20 kDa PEGDA were 10 and 20%. The concentrations for 3.4 and 5 kDa were 20 and 40%. We define the lower concentrations as 1× and the higher concentrations as 2×. The concentrations of PEGDA used are summarized in Table I. The scaffolds were fabricated using molds constructed of two 25 × 75 mm^2 precleaned glass microscope slides separated by a 500-μm Teflon spacer. The molds were disinfected with 70% ethanol and exposed to UV light (B-200SP UV lamp, UVP, 365 nm 10 mW^2/cm^2) for further sterilization for at least an hour prior to use. The prepolymer PEGDA solutions were injected into the molds through a 0.2-μm polyethersulfone syringe filter, then the molds were exposed to the UV light for 3 min. After polymerization, rectangular-shaped hydrogel scaffolds were removed from the molds with tweezers and fully immersed in 5 mL phosphate buffered saline (PBS) within petri dishes and allowed to swell for 24 h.

TABLE I. PEGDA Formulations for Hydrogel Fabrication

PEGDA Molecular Weight (kDa)	PEGDA Concentration (%w/v)	
	1×	2×
3.4	20%	40%
5	20%	40%
10	10%	20%
20	10%	20%

Characterization of elastic modulus

Elastic moduli were determined by performing tensile tests using a Bose Electroforce 3100 with a 1 Newton load cell. Hydrogel scaffolds were removed from PBS immediately prior to testing to maximize their hydration during testing. Testing lasted approximately 3 min for each scaffold, which was far less than the 20–30 min it takes for these scaffolds to dry. The hydrated hydrogels' thicknesses and the working distance between clamps were measured in mm using digital calipers. The average thicknesses of high and low modulus scaffolds were 0.61 ± 0.03 and 0.58 ± 0.05 mm, respectively. Though the differences were not statistically significant, the measured thicknesses were used to calculate the cross-sectional area of each hydrated hydrogel. Rather than using force applied to determine elastic moduli, the measured cross-sectional area values were used to determine the applied tensile stresses, which normalizes for differences in swelling ratios. Following measurement, scaffolds were clamped at either end. Bose Electroforce flat knurled face tension/compression grips were mounted vertically and the grips' inner faces were modified with duct tape to pad the surfaces. This prevented the sharp edges of the grips from pinching through the scaffolds. The scaffolds were tested in uniaxial strain applied at a rate of 6 mm/min. WinTest® 7 software was used for system control and force data acquisition. The data was collected and used to calculate the elastic modulus from the slope in the linear portion of the stress-strain curve ($n = 5$ for each molecular weight).

Synthesis of acryl-PEG-RGDS

Heterobifunctionalized Acrylate-PEG-Succinimydal Valerate (ACRL-PEG-SVA; Laysan Bio, Arab, AL) was reacted with RGDS (Tocris, Bristol, UK) in a 1:1.2 molar ratio at pH 8.0 under argon. The reaction mixture was placed on a rocker on its highest tilt and speed overnight in a 4°C cold room. Following overnight reaction, the solution was then dialyzed against 4 L of ultra pure water in a 1000 MWCO cellulose membrane (Spectrum Labs, Rancho Dominguez, CA), lyophilized, and stored at −20°C.

Confirmation of RGDS conjugation

Ninhydrin assays were performed to measure the amount of free RGDS following the conjugation reaction with ACRL-PEG-SVA. Ninhydrin reacts with free amines and produces a colored product. This colorimetric assay permits the measurement of unconjugated RGDS via reaction with free amines on the arginine. Briefly, prior to dialyzing the reaction solution, a 250-μL sample was lyophilized and reconstituted in 100 μL of PBS. This reconstituted solution was next added to 100 μL of sodium citrate buffer and 200 μL of 2% ninhydrin solution in an Eppendorf low protein binding tube. This was then placed in a boiling water bath for 15 min. Absorbance of the solution was read on a Beckman DTX 880 Multimode Detector at 570 nm. A standard curve was produced using known concentrations of RGDS.

Scaffold preparation for cell culture

Protein-modified scaffolds were fabricated using the scaffold fabrication process described above with the addition of 10 m*M* ACRL-PEG-RGDS to the polymer solution. Scaffolds were then swelled in whole culture media (described below) for 24 h, changing the media regularly for the first 8 h to allow for unconjugated peptide to be removed. For cell culture, a low modulus (60 kPa) scaffold made with 0.1 g/mL 20 kDa PEGDA and a high modulus (1200 kPa) scaffold made with 0.4 g/mL 5 kDa PEGDA were used.

Cell culture

ARPE-19 cells (ATCC, Manassas, VA) were seeded on scaffolds at 10,000 cells/cm^2. Cells were cultured in DMEM/F12 with 15% v/v fetal bovine serum and 1% v/v antibiotic solution (10,000 Units penicillin and 10 mg streptomycin per mL). Scaffolds were moved to a new well after 8 h to retain only cells attached to scaffolds and eliminate cells that attached to well bottoms. Media was changed every other day for 14 days. Cell analyses were conducted on days 1, 7, and 14.

Fluorescence microscopy

Live/Dead® calcein acetoxymethyl (AM) and ethidium homodimer-1 viability/cytotoxicity stain (Life Technologies, Carlsbad, CA) was performed to qualitatively assess cell adherence and viability. Briefly, the ethidium homodimer-1 and calcein AM was added to media in 1:500. Scaffolds were incubated in the solution for 10 minutes. Following incubation, cell nuclei were labeled using Hoescht at a 1:5000 dilution in PBS. The scaffolds were then washed in PBS and imaged ($n = 3$ for each condition) on a fluorescent microscope (Axio Observer Z1, Zeiss, Oberkochen, Germany).

Metabolic assay

PrestoBlue mitochondrial reduction assay was performed on days 1, 7, and 14 to determine cellular activity on the scaffolds of varying moduli. Control and experimental scaffolds with cells attached were immersed in assay solution and incubated for 4 h. Controls were matched molecular weight hydrogels with no cells attached. A 100 μL sample of assay solution was aspirated from each well following the incubation period and pipetted into a fresh 96 well plate then read on a Beckman Coulter DTX 880 Multimode Detector with excitation at 560 nm and emission at 595 nm. The values read for control scaffold fluorescence was subtracted from the values read for experimental scaffold fluorescence ($n = 5$ for each condition).

qPCR

ARPE-19 RNA was isolated using Qiagen RNEasy Plus kit (Qiagen, Hilden, Germany) according to the manufacturer's protocol. Briefly, cells were lysed using β-mercaptoethanol and Qiagen RLT Plus buffer and then centrifuged through a Qiashredder column to remove large debris and contaminants. Genomic DNA was removed using an eliminator column. Following this, ethanol was used to provide binding

TABLE II. Primer Sequences for Real-Time PCR

Gene of Interest	Primer Sequence (5′–3′)
CRALBP	F: AGATCTCAGGAAGATGGTGGAC
	R: GAAGTGGATGGCTTTGAACC
IL-6	F: GGCACTGGCAGAAAACAACC
	R: GCAAGTCTCCTCATTGAATCC
MCP-1	F:GATCTCAGTGCAGAGGCTCG
	R:TGCTTGTCCAGGTGGTCCAT
IL-8	F: CTGGCCGTGGCTCTCTTG
	R: CCTTGGCAAAACTGCACCTT
SMAD3	F:TCCCCAGCACATAATAACTT
	R:TGGGAGACTGGACAAAAAT
GAPDH	F: ACCACAGTCCATGCCATCAC
	R: TCCACCACCCTGTTGCTGTA

conditions for RNA to the RNeasy spin column, while other non-RNA contaminants were then washed away. The RNA was then eluted through the column and quantified using a NanoDrop^{TM} spectrophotometer and associated software. Next, the RNA was normalized to a uniform concentration. Samples were reverse transcribed using the High Capacity cDNA Reverse Transcription Kit (Applied Biostystems). PCR was performed using SYBR Green PCR Master (Applied Biosystems) mix and PikoReal real time PCR system. The primer sequences used are listed in Table II. The fold change relative gene expression compared to that of the control TCPS was determined using the delta-delta Ct method after normalizing to the housekeeping gene, *GAPDH* ($n = 5$ for each condition).

Statistical analysis

Cellular metabolic activity, elastic moduli, and gene expression were compared between the different molecular weight scaffolds using a Student's *t test* when comparing two groups or an analysis of variance (ANOVA) when comparing more than two groups. Following ANOVA, pairwise comparisons between groups was performed using Tukey's post-hoc analysis. For metabolic activity and gene expression analyses, the dependent variables were control-adjusted results. p Values <0.05 were considered significant and analyses were conducted in Matlab and Microsoft Excel. Statistical significance is reported in the figures, which are reported as mean ± standard error.

RESULTS

Mechanical characterization of scaffolds

The Young's modulus of scaffolds tested in uniaxial tension was determined following 24 hours of scaffold swelling in PBS. Scaffold modulus was modified through two approaches. The first approach was by varying the PEGDA molecular weight and the second approach was to vary to concentration of PEGDA in solution. Using molecular weights 3.4, 5, 10, and 20 kDa, the Young's modulus can be changed up to two orders of magnitude. The tested scaffolds' moduli varied between 60 and 1200 kPa. The elastic modulus for all scaffold formulations is shown in Figure 1.

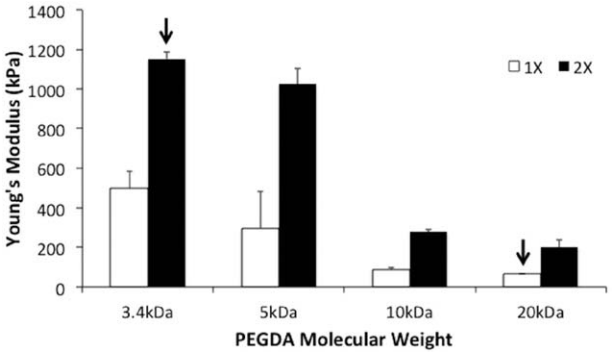

FIGURE 1. The effects of molecular weight and concentration on scaffold modulus. Higher PEGDA molecular weight leads to a lower modulus, or a less rigid scaffold. Higher concentrations of PEGDA lead to a higher modulus, or a more rigid scaffold. Arrows indicate scaffolds used in cell studies.

Fluorescent microscopy

Following the seeding of cells on low modulus (60 kPa) and high modulus (1200 kPa) scaffolds, fluorescent microscopy was performed. These images were analyzed qualitatively to observe differences in cell adhesion patterns. Representative images are shown in Figure 2. The cells show a more homogenous spreading on the high modulus scaffold compared to the low modulus scaffold. Cell clusters with a higher percentage of cell death was observed on the low modulus scaffold.

Cell activity

The metabolic activity assay was conducted on days 1, 7, and 14 of culture. Results were normalized to day 1 to determine how the cellular activity changed over the culture period. On both days 7 and 14, the high modulus scaffold results in greater cell metabolic activity than the tissue culture plastic (control) or the low modulus scaffold. On day 7, this increase over control is not significant, but on day 14 it is ($p = 0.04$). When compared to control, the low modulus scaffold reduced cell metabolic activity on both days 7 and 14, $p = 0.004$ and 0.001, respectively. It should be noted that there was no noticeable difference in the number of cells on each substrate over the 14 days. After14 days, the cells on the high modulus scaffold were the only cells with an increase in metabolic activity over day 1 (Fig. 3).

Gene expression

The genes investigated in this work can be categorized into three categories: inflammation, dedifferentiation, and function. The expression of IL-6 and MCP-1, the inflammatory microglial migration genes, was increased on both scaffold moduli relative to TCPS. The expression of IL-6 and IL-8 on the high modulus scaffold was significantly higher ($p = 0.02$ and 0.01, respectively) than on the low modulus scaffold. The functional gene, CRALBP, demonstrated a downregulation on both scaffolds compared to the TCPS. Lastly, the dedifferentiation gene, SMAD3, showed slight non-significant increases on scaffold surfaces relative to the control (Fig. 4).

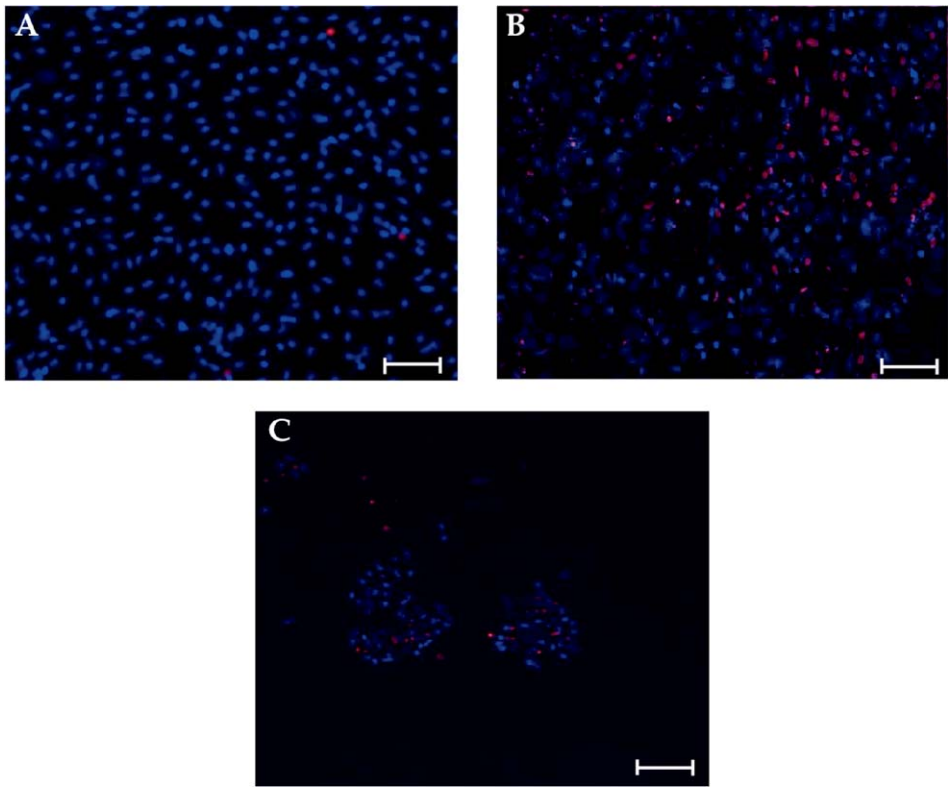

FIGURE 2. ARPE-19 cells on different culture substrates. The ARPE-19 cells formed a confluent monolayer on TCPS with very little cell death (A); the cells still had a high density on the high modulus scaffold, with more noticeable cell death (B); cells formed clumps on the low modulus scaffolds with cell death on the low modulus scaffolds (C). Blue = Hoescht, Nuclear Stain; Red = ethidium homodimer-1, dead cells. Scale bar 100 μm.

DISCUSSION

This study demonstrates that the Young's modulus of a scaffold has significant effects on RPE cells. Previously published RPE studies on scaffolds have demonstrated microglial migration and the presence of fibroblast- and macrophage-like cells following implantation. Since IL-6 and MCP-1 are microglial attractants and SMAD3 is the pathway that has been implicated in RPE dedifferentiation into fibroblast- and microphage-like phenotypes, we focused our study on how scaffold modulus affects the expression these genes in the seeded RPE cells. The expression of IL-6 on the high modulus, a statistically significant 3-fold increase

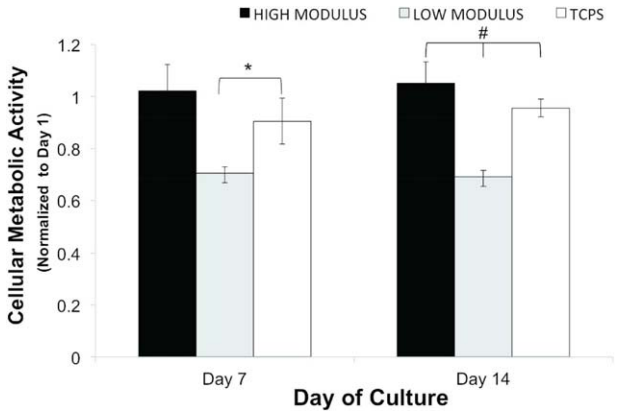

FIGURE 3. Cell metabolic activity on scaffolds of varying modulus. By day 7 of culture, the cells on the low modulus scaffold had significantly decreased activity when compared to both other conditions. The high modulus and TCPS were not different on day 7. On day 14, all three groups were significantly different with the high modulus scaffold having the highest activity. $^{*}p < 0.01$; $^{\#} < 0.05$.

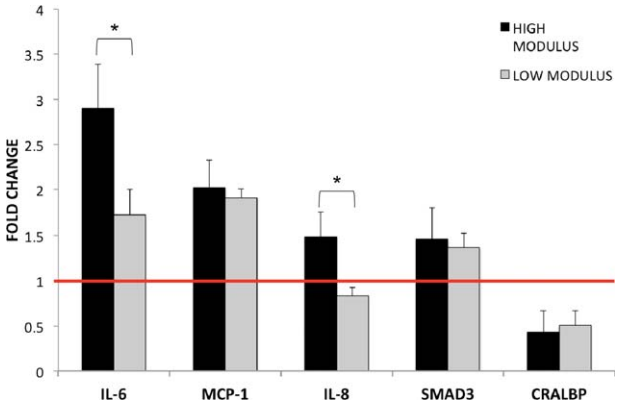

FIGURE 4. Relative gene expression of cells on two different modulus scaffolds. Microglial attractants, IL-6 and MCP-1, both demonstrated upregulation on the elastic scaffold substrates compared to TCPS (TCPS expression is represented by the red line) SMAD3, a dedifferentiation marker is slightly upregulated on the scaffolds, while CRALBP, a characteristic RPE gene is downregulated. $^{*}p < 0.05$.

relative to control TCPS and 1.5-fold higher than the low modulus scaffold, suggests that this scaffold could contribute to recruiting microglia *in vivo*. In addition, both scaffolds demonstrated almost a 2-fold increase in MCP-1, another microglial attractant, expression relative to control TCPS. These results demonstrate the importance of modulus as a design parameter for scaffolds to be used for RPE transplantation. Through careful design and fabrication of scaffolds, it is possible to control scaffold modulus and, therefore, may be possible to control the expression of these microglial attractants for successful long-term treatment.

Fluorescent microscopy qualitatively revealed that RPE cells had different adhesion patterns on low modulus and high modulus scaffolds. This is a significant observation because early studies on the effects of scaffold modulus on epithelial cells suggest that cells sense their physical environment, causing differences in focal adhesions and expression of intracellular pathways. RPE dedifferentiation has been characterized by a change in expression of cytokeratin proteins, a component of the intracellular cytoskeleton. Therefore, it is possible that the mechanical environment experienced by RPE cells affects their adhesion and initiates or promotes dedifferentiation. This is supported by recent work demonstrating difference in phagocytic ability of RPE cells on different substrate moduli.[31]

The cell activity, as measured by a mitochondrial reduction assay, varied on the different moduli. Because it remains difficult to quantify cell number on scaffolds, the cell activity was normalized to the day 1 activity. Therefore, changes in activity can be attributed to either cell number due to proliferation or death, or change in the cell activity itself. By day 7, the cells cultured on low modulus scaffolds had an activity approximately 70% of their day 1 activity. The cells cultured on the high modulus scaffold increased their activity over the 14-day culture period to a level statistically different from the other two groups. This demonstrates that either proliferation is occurring on the high modulus scaffold or the cells are more metabolically active.

For the first time, this study reveals the response of RPE cells to changes in scaffold modulus. We demonstrated that the modulus of a substrate affects the expression of the microglial attractants, IL-6 and MCP-1. This establishes that scaffold modulus should be considered an important design parameter in scaffolds developed for RPE transplantation. We were able to promote the expression of the IL-6 and MCP-1 inflammatory genes in RPE cells simply by altering the mechanical properties of the underlying scaffolds. If scaffold mechanical properties alone can promote the expression of these inflammatory genes *in vitro*, it is reasonable to believe that once implanted into a diseased retina, the inflammatory response will be significant. While we did not see overexpression of SMAD3 in our study, we do believe that the mechanical environment can encourage RPE dedifferentiation and should be further investigated. Although, we did not see significant difference in the gene expression between the two scaffold groups, this could be because the difference in scaffold moduli was not great enough. This is supported by significant differences seen between the scaffolds and the control TCPS, which has been reported to have a modulus in the gigapascal range.[32]

This study demonstrates that modulus is an important design parameter for scaffolds designed for RPE cell transplantation. It is particularly important to consider how the mechanical environment affects the RPE phenotype and expression of inflammatory markers, as these are two challenges RPE scaffolds faces in the translation of cell therapies. Further investigation is needed to fully tease out the effects of modulus and move toward scaffold design optimization.

REFERENCES

1. Hill D. Age-related macular degeneration. InnovAiT: Education and Inspiration for General Practice 2015;8:425–430.
2. Age-Related Eye Disease Study 2 Research, G. Lutein + zeaxanthin and omega-3 fatty acids for age-related macular degeneration: the Age-Related Eye Disease Study 2 (AREDS2) randomized clinical trial. JAMA 2013;309:2005–2015.
3. Alexander P, Thomson HA, Luff AJ, Lotery AJ. Retinal pigment epithelium transplantation: concepts, challenges, and future prospects. Eye 2015;29:992–1002 (Lond)
4. Li LX, Turner JE. Transplantation of retinal pigment epithelial cells to immature and adult rat hosts: short- and long-term survival characteristics. Exp Eye Res 1988;47:771–785.
5. Li LX, Turner JE. Inherited retinal dystrophy in the RCS rat: prevention of photoreceptor degeneration by pigment epithelial cell transplantation. Exp Eye Res 1988;47:911–917.
6. Lopez R, Gouras P, Kjeldbye H, Sullivan B, Reppucci V, Brittis M, Wapner F, Goluboff E. Transplanted retinal pigment epithelium modifies the retinal degeneration in the RCS rat. Invest Ophthalmol Vis Sci 1989;30:586–588.
7. Wang S, Lu B, Wood P, Lund RD. Grafting of ARPE-19 and Schwann cells to the subretinal space in RCS rats. Invest Ophthalmol Vis Sci 2005;46:2552–2560.
8. Binder S, Stanzel BV, Krebs I, Glittenberg C. Transplantation of the RPE in AMD. Prog Retin Eye Res 2007;26:516–554.
9. Lu B, Malcuit C, Wang S, Girman S, Francis P, Lemieux L, Lanza R, Lund R. Long-term safety and function of RPE from human embryonic stem cells in preclinical models of macular degeneration. Stem Cells 2009;27:2126–2135.
10. Curcio CA, Johnson M. Structure, function, and pathology of Bruch's membrane. Elastic 2013;146:210–213.
11. Gullapalli VK, Sugino IK, Van Patten Y, Shah S, Zarbin MA. Impaired RPE survival on aged submacular human Bruch's membrane. Exp Eye Res 2005;80:235–248.
12. Gullapalli VK, Sugino IK, Van Patten Y, Shah S, Zarbin MA. Retinal pigment epithelium resurfacing of aged submacular human Bruch's membrane. Trans Am Ophthalmol Soc 2004;102:123–137. discussion 137-8.
13. Bhatt NS, Newsome DA, Fenech T, Hessburg TP, Diamond JG, Miceli MV, Kratz KE, Oliver PD. Experimental transplantation of human retinal pigment epithelial cells on collagen substrates. Am J Ophthalmol 1994; 117:214–221.
14. Lu L, Yaszemski MJ, Mikos AG. Retinal pigment epithelium engineering using synthetic biodegradable polymers. Biomaterials 2001;22:3345–3355.
15. Lee CJ, Vroom JA, Fishman HA, Bent SF. Determination of human lens capsule permeability and its feasibility as a replacement for Bruch's membrane. Biomaterials 2006;27:1670–1678.
16. Lu B, Zhu D, Hinton D, Humayun MS, Tai YC. Mesh-supported submicron parylene-C membranes for culturing retinal pigment epithelial cells. Biomed Microdevices 2012;14:659–667.
17. Hynes SR, Lavik EB. A tissue-engineered approach towards retinal repair: scaffolds for cell transplantation to the subretinal space. Graefes Arch Clin Exp Ophthalmol 2010;248:763–778.
18. Liu Z, Yu N, Holz FG, Yang F, Stanzel BV. Enhancement of retinal pigment epithelial culture characteristics and subretinal space tolerance of scaffolds with 200 nm fiber topography. Biomaterials 2014;35:2837–2850.

19. He W, McConnell GC, Bellamkonda RV. Nanoscale laminin coating modulates cortical scarring response around implanted silicon microelectrode arrays. J Neural Eng 2006;3:316–326.
20. Tang L, Eaton JW. Inflammatory responses to biomaterials. Am J Clin Pathol 1995;103:466–471.
21. Saika S, Kono-Saika S, Tanaka T, Yamanaka O, Ohnishi Y, Sato M, Muragaki Y, Ooshima A, Yoo J, Flanders KC, Roberts AB. Smad3 is required for dedifferentiation of retinal pigment epithelium following retinal detachment in mice. Lab Invest 2004;84:1245–1258.
22. Oganesian A, Gabrielian K, Ernest JT, Patel SC. A new model of retinal pigment epithelium transplantation with microspheres. Arch Ophthalmol 1999;117:1192–1200.
23. Del Priore LV, Tezel TH, Kaplan HJ. Survival of allogeneic porcine retinal pigment epithelial sheets after subretinal transplantation. Invest Ophthalmol Vis Sci 2004;45:985–992.
24. Christiansen AT, Tao SL, Smith M, Wnek GE, Prause JU, Young MJ, Klassen H, Kaplan HJ, la Cour M, Kiilgaard JF. Subretinal implantation of electrospun, short nanowire, and smooth poly(epsilon-caprolactone) scaffolds to the subretinal space of porcine eyes. Stem Cells Int 2012;2012:454295. p.
25. Saha K, Keung AJ, Irwin EF, Li Y, Schaffer DV, Healy KE. Substrate modulus directs neural stem cell behavior. Biophys J 2008;95:4426–4438.
26. Banerjee A, Arha M, Choudhary S, Ashton RS, Bhatia SR, Schaffer DV, Kane RS. The influence of hydrogel modulus on the proliferation and differentiation of encapsulated neural stem cells. Biomaterials 2009;30:4695–4699.
27. Evans ND, Minelli C, Gentleman E, LaPointe V, Patankar SN, Kallivretaki M, Chen X, Roberts CJ, Stevens MM. Substrate stiffness affects early differentiation events in embryonic stem cells. Eur Cell Mater 2009;18:1–13. discussion 13-4.
28. Discher DE, Janmey P, Wang YI. Tissue Cells Feel and Respond to the Stiffness of Their Substrate. Science 2005; 310:1139–1143.
29. Pelham RJ, Wang YI. Cell locomotion and focal adhesions are regulated by substrate flexibility. Proc Natl Acad Sci USA 1997;94:13661–13665.
30. Zhu J. Bioactive modification of poly(ethylene glycol) hydrogels for tissue engineering. Biomaterials 2010;31:4639–4656.
31. Boochoon KS, Manarang JC, Davis JT, McDermott AM, Foster WJ. The influence of substrate elastic modulus on retinal pigment epithelial cell phagocytosis. J Biomech 2014;47:3237–3240.
32. Gilbert PM, Havenstrite KL, Magnusson KE, Sacco A, Leonardi NA, Kraft P, Nguyen NK, Thrun S, Lutolf MP, Blau HM. Substrate elasticity regulates skeletal muscle stem cell self-renewal in culture. Science 2010;329:1078–1081.